CEREBELLAR NEURONAL DYSFUNCTION ACCOMPANIES EARLY MOTOR SYMPTOMS IN SPINOCEREBELLAR ATAXIA TYPE 3 AND IS PARTIALLY ALLEVIATED UPON CHRONIC CITALOPRAM TREATMENT

Palarz KJ*[1], Neves-Carvalho A*[1,2,3], Duarte-Silva S[2,3], Maciel P[2,3], Khodakhah K[1]

*co-first

[1]Dominick P. Purpura Department of Neuroscience, Albert Einstein College of Medicine, Bronx, NY 10461
[2]Life and Health Sciences Research Institute (ICVS), School of Medicine, University of Minho, Braga, Portugal
[3]ICVS/3B's – PT Government Associate Laboratory, Braga/Guimarães, Portugal

ABSTRACT

Spinocerebellar ataxia type 3 (SCA3) is an adult-onset, progressive ataxia with no current disease modifying treatments. SCA3 patients have mild degeneration of the cerebellum, a brain area involved in motor coordination and maintenance of balance, as well as of the brainstem, of the spinal cord and of other movement-related subcortical areas. However, both SCA3 patients and SCA3 mouse models present clinical symptoms before any gross pathology is detectable, which suggests neuronal dysfunction precedes neurodegeneration, and opens an opportunity for therapeutic intervention. Such observations also raise the question of what triggers these abnormal motor phenotypes. Purkinje cells are the major computational unit within the cerebellum and are responsible for facilitating coordinated movements. Abnormal Purkinje cell activity is sufficient to cause ataxia. In this study, we show that the CMVMJD135 mouse model of SCA3 has dysfunctional deep cerebellar nuclei and Purkinje cells. Both cell types have increased irregularity as measured by inter-spike interval coefficient of variation. Purkinje cell dysfunction is likely a combination of intrinsic and extrinsic (synaptic) dysfunction. Interestingly, Citalopram, a selective serotonin reuptake inhibitor previously shown to alleviate disease in CMVMJD135 mice, also improved cerebellar neuron function in the CMVMJD135 mouse model. Specifically, we found that Purkinje cell dysfunction when synaptic transmission is intact was alleviated with citalopram treatment, however, intrinsic Purkinje cell dysfunction was not alleviated. Altogether, our findings suggest that cerebellar neuronal dysfunction contributes to the onset of SCA3 motor dysfunction and that citalopram, while effective at alleviating the motor phenotype, does not restore Purkinje cell intrinsic activity in SCA3. A novel therapeutic approach that combines citalopram with another therapeutic that targets this intrinsic dysfunction in a complementary manner might further reduce disease burden in SCA3.

INTRODUCTION

The cerebellum is involved in motor coordination and maintenance of balance. Dysfunction of the cerebellum leads to ataxia, or uncoordinated movement. The most common dominantly inherited ataxia is Spinocerebellar ataxia type 3 (SCA3), also known as Machado-Joseph Disease (MJD). SCA3 is caused by a heterozygous CAG repeat expansion of the Ataxin-3 gene (Kawaguchi *et al.*, 1994). Patients present with adult-onset progressive ataxia, along with a combination of ophthalmoplegia, spasticity, dystonia, muscular atrophy, or other extrapyramidal signs (Coutinho & Andrade, 1978; Barbeau *et al.*, 1984). The most common affected regions on pathology include the cerebellar dentate nucleus, pallidum, substantia nigra, thalamus, subthalamic nuclei, red nuclei, and, to a lesser extent, the cerebellar cortex (Woods & Schaumburg, 1972; Rosenberg *et al.*, 1976; Romanul *et al.*, 1977; Stefanescu *et al.*, 2015; Hernandez-Castillo *et al.*, 2018; Koeppen, 2018; Wang *et al.*, 2020). Degeneration and other pathologic hallmarks, such as protein aggregate formation, occur fairly late in the course of the disease. In the cerebellum of SCA3 patients, pathology has consistently shown late-onset degeneration of the deep cerebellar nuclei, the main output of the cerebellum, but little to no degeneration of the Purkinje cells, the main computational unit of the cerebellar cortex (Rosenberg *et al.*, 1976; Haines & Dietrichs, 2012; Koeppen, 2018).

Patients with SCA3 are heterozygous for the (CAG)n/polyglutamine expansion in ATXN3 a protein that is ubiquitously expressed in all cell types in the body. A SCA3 mouse model (CMVMJD135) expresses the expanded disease-relevant ataxin-3c isoform under the human cytomegalovirus (CMV) promoter in a heterozygous manner, conferring wide expression at near endogenous levels throughout the nervous system, similar to what is seen in patients (Silva-Fernandes *et al.*, 2014; Teixeira-Castro *et al.*, 2015). As with other CAG repeat expansion disorders, the repeat length is longer in the mouse model compared to SCA3 patients (Silva-Fernandes *et al.*, 2014; Teixeira-Castro *et al.*, 2015; Arteaga-Bracho *et al.*, 2016). Despite this, the mouse model recapitulates the adult onset, progressive motor phenotypes seen in SCA3

patients, neuropathological findings, in addition to a late in disease neuronal degeneration profile with sparing of Purkinje cells.

There are few therapies available for treatment of ataxia, with limited efficacy. Serotonergic drugs have historically been the most promising, with SCA3 patients exhibiting the most consistent benefits among ataxia patients (Plaitakis *et al.*, 1978; Trouillas *et al.*, 1988; Trouillas *et al.*, 1995; Trouillas *et al.*, 1997; Takei *et al.*, 2002; Takei *et al.*, 2004; Takei *et al.*, 2005; Takei *et al.*, 2010). The CMVMJD135 mouse model is also responsive to a serotonergic agent, citalopram, a selective serotonin reuptake inhibitor (Teixeira-Castro *et al.*, 2015; Esteves *et al.*, 2019). As cerebellar dysfunction is a key player in ataxia, it is plausible that these agents are acting on cerebellar activity. Serotonergic fibers are present throughout the cerebellum, with several of the 14 serotonin receptors being expressed throughout the cerebellum (Bishop & Ho, 1985; Kerr & Bishop, 1991; Kitzman & Bishop, 1994; Dieudonne, 2001; Oostland & van Hooft, 2013). While it is unknown exactly how serotonin is modulating cerebellar activity, serotonin can affect many aspects of the cerebellar circuit, including Purkinje cell activity, synaptic transmission, and deep cerebellar nuclei activity (Strahlendorf & Hubbard, 1983; Strahlendorf *et al.*, 1984; Strahlendorf *et al.*, 1986; Darrow *et al.*, 1990; Dieudonne, 2001; Dean *et al.*, 2003; Saitow *et al.*, 2009; Murano *et al.*, 2011; Zhang *et al.*, 2014; Lippiello *et al.*, 2016). Disruption to the regularity of firing of Purkinje cells and deep cerebellar nuclei neurons is found in many mouse models of ataxia and is proposed to cause many forms of ataxia (Ito, 1984; Walter *et al.*, 2006; Alvina & Khodakhah, 2010b; a; Hourez *et al.*, 2011; Shakkottai *et al.*, 2011; Hansen *et al.*, 2013; Tempia *et al.*, 2015; Hoxha *et al.*, 2018; Tara *et al.*, 2018). Together with the understanding that ataxia arises from cerebellar dysfunction, the alleviation of motor symptoms upon citalopram administration to the CMVMJD135 mouse prompted us to ask whether citalopram targeted cerebellar activity in order to alleviate the motor dysfunction in SCA3.

Using the CMVMJD135 mouse model (referred to as SCA3 mice throughout this paper) we demonstrate that Purkinje cells and deep cerebellar nuclei neurons have abnormal, irregular

firing early in the course of the disease before pathology is detected. We observed that the dysfunction of Purkinje cells was partially restored upon chronic citalopram treatment, but the intrinsic dysfunction was not alleviated. Overall, this suggests Purkinje cell intrinsic activity as a therapeutic target to use as adjunctive therapy with citalopram in SCA3.

RESULTS

SCA3 mice have motor dysfunction early in disease

To better characterize the motor phenotype of the SCA3 mice to be used in this study across the course of the disease, we used some established tests of motor performance. We first assessed the SCA3 mice and littermate wild-types (referred to as wild-type throughout this paper) on the previously published disability scale for gross motor abnormalities (Weisz *et al.*, 2005; Tara *et al.*, 2018). Using this scale, a mouse with no motor symptoms receives a score of 0, a 1 indicates abnormal gait, and the severity of motor impairment scales up to a score of 5 (Figure 1A). SCA3 mice had minor motor impairment at 12 weeks of age (wild-type 0.17±0.14, SCA3 0.52±0.28, $p=0.0018$), with overt impairment at 34 weeks (wild-type 0.19±0.17, SCA3 1.70±0.58, $p<0.001$) and severe impairment by 60 weeks (wild-type 0.27±0.16, SCA3 2.63±0.10, $p<0.001$) when compared to wild-type mice (Figure 1B). This demonstrates the progressive nature of the disease in SCA3 mice. By 60 weeks, the motor symptoms likely represent the combination of deficits from throughout the central and peripheral nervous system (Silva-Fernandes *et al.*, 2010; Duarte-Silva *et al.*, 2014; Silva-Fernandes *et al.*, 2014; Teixeira-Castro *et al.*, 2015; Esteves *et al.*, 2019).

The second assay, the parallel rod floor test, is more sensitive to motor incoordination and eliminates variability due to human error compared to the disability score (Kamens *et al.*, 2005; Kamens & Crabbe, 2007). The ataxia index (Figure 1C), calculated by number of errors, or foot slips (Figure 1D), per distance traveled (cm) (Figure 1E), was averaged per mouse over two trials. SCA3 mice had a higher ataxia index than wild-types as early as 12 weeks of age (wild-type

0.074±0.029, SCA3 0.202±0.083, p<0.001), with the ataxia index further increasing at 34 weeks (wild-type 0.112±0.023, SCA3 0.476±0.211, p<0.001) and 60 weeks of age (wild-type 0.111±0.035, SCA3 1.645±1.51, p<0.001) (Figure 1). This increase is likely due to a combination of increased central and peripheral dysfunction. Nonetheless, the parallel rod floor test provides a sensitive measure of motor impairment in SCA3 mice as early as 12 weeks of age, an age at which no central pathology has been detected (Silva-Fernandes *et al.*, 2014; Teixeira-Castro *et al.*, 2015; Esteves *et al.*, 2019).

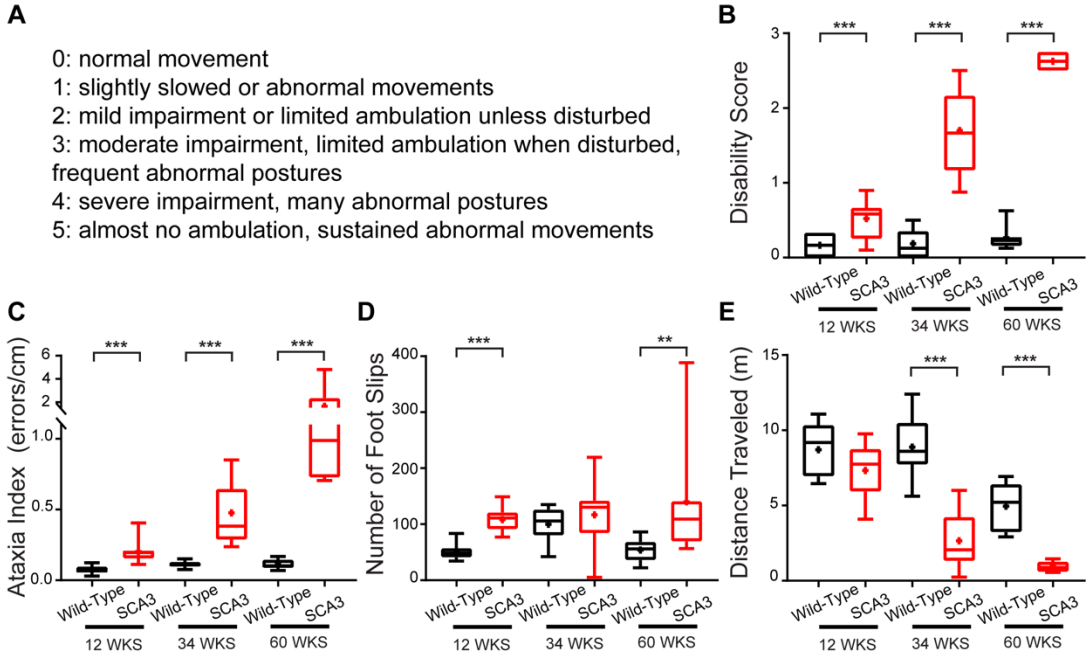

Figure 1: SCA3 motor symptoms progress with age, with an onset as early as 12 weeks. SCA3 mice and wild-types were tested at 12, 34, and 60 weeks of age on the disability score (A-B) and parallel rod floor test (C-E). (A-B) SCA3 mice have an increased disability score (A) compared to wild-types at 12 weeks, and the score progresses with age. (C-E) SCA3 mice have an increased ataxia index (C) at 12 weeks due to increased foot slips (D) with no change in distance traveled (E). At 34 and 60 weeks of age, the increased ataxia index likely reflects combined decrease in distance traveled and increased foot slips.
Parallel Rod Floor Test: 12 weeks wild-type N = 9, SCA3 N = 9. 34 weeks wild-type N = 8, SCA3 N = 9. 60 weeks wild-type N = 8, SCA3 N = 7. Disability Score (all mice were observed twice, and scores were averaged): 12 weeks wild-type N = 10, SCA3 N = 15. 34 weeks wild-type N = 17, SCA3 N = 19. 60 weeks wild-type N = 8, SCA3 N = 7.

Neuronal activity of the cerebellar output nuclei is impaired in SCA3 mice

One of the most consistently affected regions in SCA3 patients is the deep cerebellar nuclei (DCN), which form the main output of the cerebellum (Woods & Schaumburg, 1972;

Rosenberg *et al.*, 1976; Seidel *et al.*, 2012a; Seidel *et al.*, 2012b). DCN neurons fire spontaneously with a regular pattern in the absence of synaptic input, and dysfunction of DCN disrupts motor behavior (Ito, 1984; Fremont *et al.*, 2014; Tara *et al.*, 2018). It is likely that the DCN undergoes a period of dysfunction before degeneration in SCA3.

To determine if SCA3 mice have altered DCN activity, SCA3 and wild-type mice were implanted with titanium brackets for awake, head-fixed, single-unit recordings of DCN neurons (Tara *et al.*, 2018). The inter-spike interval coefficient of variation (ISI CV), a measure of spike

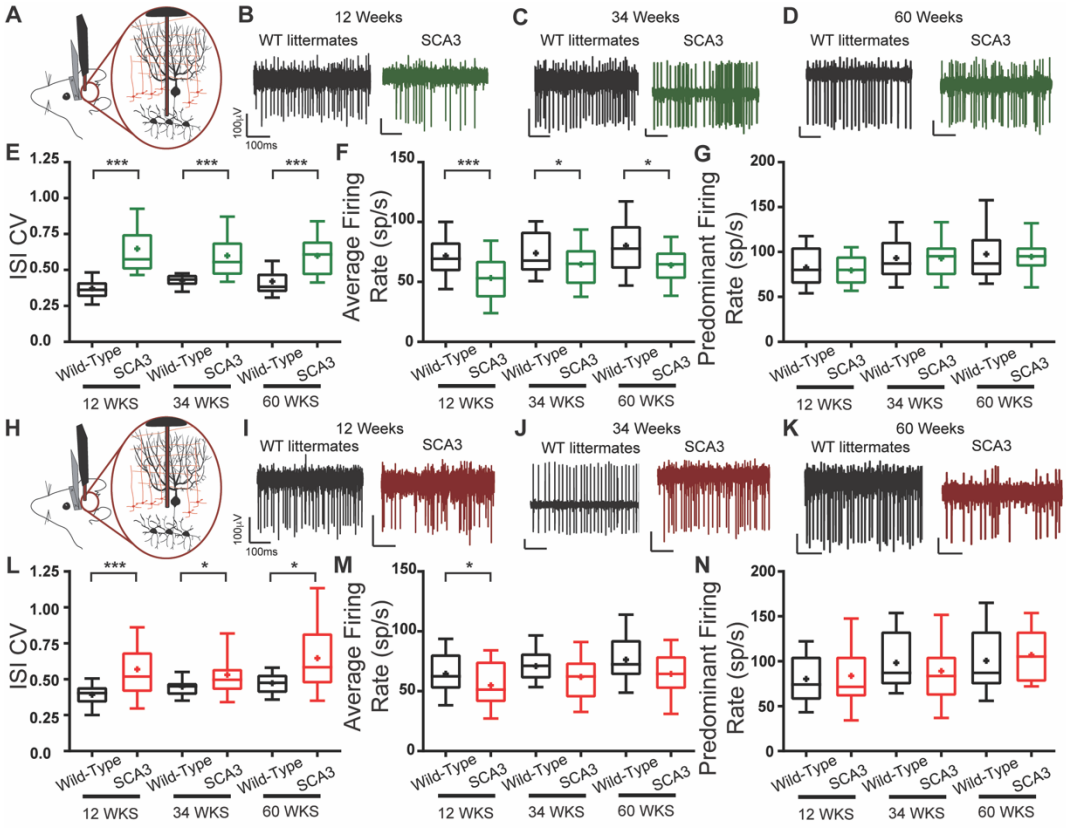

Figure 2: Cerebellar Neuronal Dysfunction in SCA3 mice across disease progression. *In Vivo* awake, head-fixed cerebellar single-unit recordings were performed from SCA3 mice and wild-types at 12, 34, and 60 weeks of age. Example deep cerebellar nuclei (A) firing traces from WT (black) and SCA3 (green) at 12 (B), 34 (C), and 60 (D) weeks of age. Deep cerebellar nuclei inter-spike interval coefficient of variation (ISI CV) (E) is increased in SCA3 while the average firing rate (F) is decreased, with no change in predominant firing rate (G) for all ages tested. Example Purkinje cell (H) firing traces from WT (black) and SCA3 (red) at 12 (I), 34 (J), and 60 (K) weeks of age. Purkinje cells ISI CV (L) is increased in SCA3 while the average firing rate (M) is decreased, with no change in predominant firing rate (N) at all ages examined. (A) and (H) are diagrams depicting recording from the DCN or Purkinje cell layer, respectively.

Deep Cerebellar Nuclei: 12 weeks wild-type N = 6, n = 39; SCA3 N = 8, n = 33. 34 weeks wild-type N = 12, n = 33; SCA3 N = 16, n = 65. 60 weeks wild-type N = 5, n = 24; SCA3 N = 3, n = 25. Purkinje cells: 12 weeks wild-type N = 6, n = 36; SCA3 N = 8, n = 32. 34 weeks wild-type N = 12, n = 29; SCA3 N = 16, n = 40. 60 weeks wild-type N = 5, n = 25; SCA3 N = 5, n = 25.

regularity, is the standard deviation of the inter-spike interval divided by the average inter-spike interval. The larger the ISI CV, the more irregular the firing. A loss of firing precision, or irregularity, can cause ataxia (Walter *et al.*, 2006). In SCA3 mice, the ISI CV of DCN was increased at 12, 34, and 60 weeks of age (12 weeks: wild-type 0.371±0.114, SCA3 0.648±0.199, $p<0.001$; 34 weeks: wild-type 0.427±0.054, SCA3 0.599±0.170, $p<0.001$; 60 weeks: wild-type 0.421±0.121, SCA3 0.599±0.152, $p<0.001$) (Figure 2E). DCN neurons had a decreased average firing rate (the reciprocal of the average inter-spike interval) at 12, 34, and 60 weeks of age in SCA3 mice compared with controls (12 weeks: wild-type 71.9±18.9, SCA3 53.4±21.5, $p<0.001$; 34 weeks: wild-type 74.1±19.8, SCA3 64.7±19.8, $p=0.0359$; 60 weeks: wild-type 80.3±26.0, SCA3 63.9±19.2, $p=0.0154$) (Figure 2F). The decrease in average firing rate would be expected to result in a decreased ISI CV if the firing pattern has not changed. Therefore, the increased ISI CV in SCA3 mice is actually higher. It is interesting to note that while the ISI CV was increased at all timepoints, there was no progressive increase in this parameter, suggesting extra-cerebellar contributions to the progressive phenotype of SCA3 mice.

Purkinje cell activity is irregular in SCA3 mice

Purkinje cells, the sole output of the cerebellar cortex, converge onto the DCN, ultimately affecting the output of the cerebellum, making it plausible that the abnormal DCN activity is driven by abnormal Purkinje cell activity (Ito *et al.*, 1970; Palay & Chan-Palay, 1974; Haines & Dietrichs, 2012; Person & Raman, 2012; White & Sillitoe, 2013). In addition, many mouse models of ataxia demonstrate abnormal firing of Purkinje cells as a source of dysfunction (Walter *et al.*, 2006; Alvina & Khodakhah, 2010b; a; Hourez *et al.*, 2011; Shakkottai *et al.*, 2011; Hansen *et al.*, 2013; Tempia *et al.*, 2015; Hoxha *et al.*, 2018; Tara *et al.*, 2018; Cook *et al.*, 2020). To determine if Purkinje cell activity is altered in SCA3, Purkinje cells were recorded from awake, head fixed SCA3 and wild-type mice. At 12, 34, and 60 weeks old, Purkinje cells in SCA3 mice had an increased ISI CV compared to wild-types (12 weeks: wild-type 0.392±0.113, SCA3 0.570±0.261,

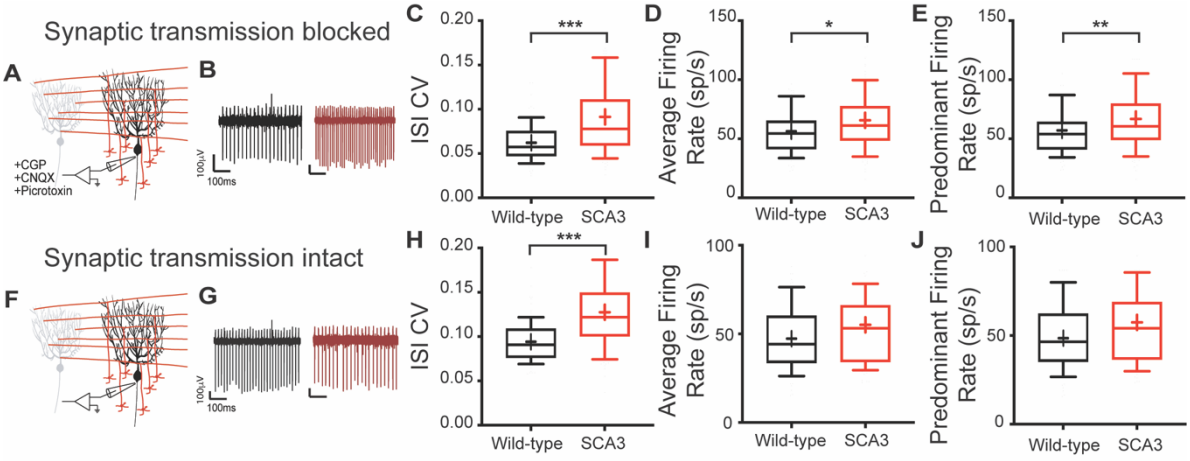

Figure 3: Purkinje cells are irregular in SCA3 mice at 34 weeks when fast synaptic transmission is blocked and intact.
In Vitro extracellular single-unit recordings were performed from SCA3 mice and wild-types at 34 weeks of age. Blockers of fast synaptic transmission (A-E) was present in the bath. Example Purkinje cell intrinsic firing traces from WT (black) and SCA3 (red) (B). Purkinje cells ISI CV (C) is increased in SCA3 with an increased average (D) and predominant (E) firing rate. Synaptic transmission was left intact, with no blockers in the bath (F-J). Example Purkinje cell intrinsic firing traces from WT (black) and SCA3 (red) with synaptic transmission intact (G). Purkinje cells inter-spike interval coefficient of variation (ISI CV) (H) is increased in SCA3 with no change in average firing rate (I) or predominant firing rate (J). Synaptic transmission blocked: WT N = 13, n = 92; SCA3 N = 15, n = 121. Synaptic transmission intact: WT N = 16, n = 89; SCA3 N = 17, n = 91.

p<0.0001; 34 weeks: wild-type 0.448±0.077, SCA3 0.531±0.183, p=0.0330; 60 weeks: wild-type 0.472±0.080, SCA3 0.646±0.262, p=0.0112), indicating irregularity of firing in SCA3 Purkinje cells (Figure 2L). Similar to the deep cerebellar nuclei, Purkinje cells in 12 weeks old SCA3 mice had a decreased average firing rate compared to wild-types, with a trend to decrease at 34 and 60 weeks (12 weeks: wild-type 64.6±19.2, SCA3 54.9±20.5, p=0.0468; 34 weeks: wild-type 71.0±16.3, SCA3 61.9±20.7, p=0.0541; 60 weeks: wild-type 76.3±24.8, SCA3 64.4±21.2, p=0.0741) (Figure 2M). With the observed decrease in average firing rate, this increased ISI CV likely represents a more pronounced irregularity of Purkinje cells.

This irregularity can be driven by a number of sources, including synaptic or intrinsic dysfunction. Purkinje cells are intrinsically active and have a very regular firing pattern when devoid of synaptic input (Raman & Bean, 1999). Our lab has previously shown that alterations in the intrinsic firing of Purkinje cells can cause ataxia (Walter *et al.*, 2006). To investigate the cause of Purkinje cell dysfunction, acute sagittal cerebellar sections were obtained from 34-week-old mice and extracellular single-unit recordings were made from visually identified Purkinje cells.

Purkinje cell intrinsic activity was determined by blocking fast synaptic transmission with $GABA_A$, $GABA_B$, and AMPA/Kainate inhibitors. The ISI CV of Purkinje cells from SCA3 mice was increased compared to wild-type mice (wild-type: 0.0623±0.022, SCA3: 0.0914±0.482, $p<0.001$) (Figure 3C). The average firing rate of intrinsic Purkinje cell activity was also increased in SCA3 mice (wild-type: 56.5±20.6, SCA3: 65.6±28.0, $p=0.0113$) (Figure 3D). The increased average firing rate suggests that the intrinsic firing rate is contributing to the increase in ISI CV but is unlikely to be the only contributing factor.

Sensorimotor integration in the cerebellum occurs via the glutamatergic and GABAergic inputs onto Purkinje cells. To determine whether firing irregularity in SCA3 mice also extended to the synaptic inputs onto Purkinje cells, we recorded extracellularly from Purkinje cells as described above, but without any blockers present in the bath, leaving synaptic transmission intact (Figure 3F-J). In this condition, where synaptic transmission is left intact, the average firing rate was not changed (wild-type: 47.3±17.6, SCA3: 55.2±26.8, $p=0.0743$) (Figure 3I) while the ISI CV was significantly increased at 0.1277±0.0439 in SCA3 compared to 0.0942±0.0239 in wild-types ($p<0.001$) (Figure 3H). Taking both *in vitro* assays together, this suggests both a synaptic and intrinsic component to Purkinje cell dysfunction in SCA3 mice.

Chronic Citalopram Treatment improves motor coordination

Chronic treatment with citalopram, a selective serotonin reuptake inhibitor, was previously shown to delay disease onset and decreases symptom severity in the SCA3 mouse line used in this study, and to have a beneficial impact on motor phenotype and mutant protein aggregation in other transgenic models of the disease (Teixeira-Castro *et al.*, 2015; Ashraf *et al.*, 2019; Esteves *et al.*, 2019). As our results demonstrate prominent cerebellar neuronal dysfunction, we sought to determine if citalopram acts through a cerebellar mechanism to improve behavior. Starting at 5 weeks of age, SCA3 and wild-type mice were either given normal drinking water or 8mg/kg citalopram in the drinking water. Mice of both sexes were tested weekly using established

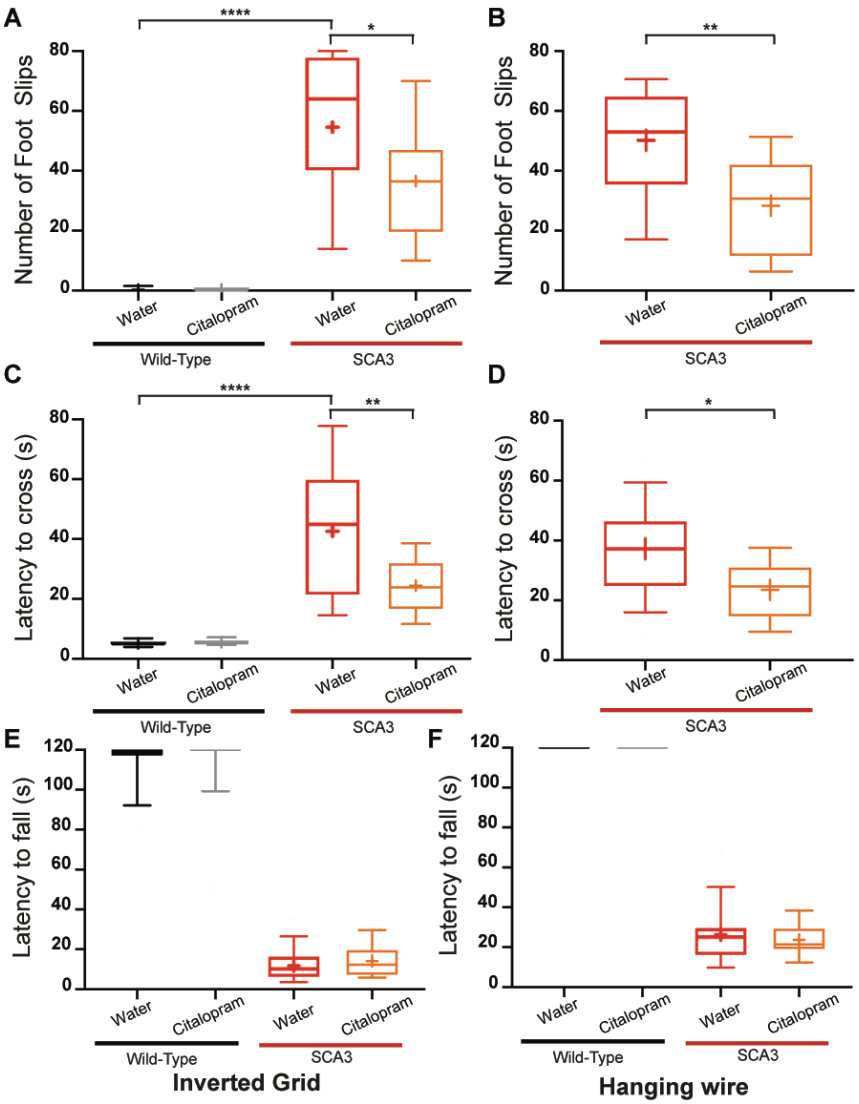

Figure 4: SCA3 motor performance improves with chronic citalopram treatment. SCA3 and wild-type mice were tested 22 weeks of age on a 1m long 2.2 cm wooden balance beam. Number of foot slips (A) (max score = 80) and latency to cross (C) on one trial, demonstrating improved performance with citalopram treatment in SCA3, and no change in wild-type mice. These results were validated on a separate day in SCA3 mice as an average of 3 trials (B, D). Grip strength was assessed as the best of 3 trials and a maximum score of 120s on the inverted grid assay (E) and the hanging wire test (F), demonstrating no improved grip strength in SCA3 with citalopram treatment.
Male mice: WT: water N = 14, citalopram N = 16; SCA3: water N = 15, citalopram N = 14.

behavioral tests which confirmed disease progression with age (Supplemental Figure 1). As there was no sex difference, only male mice were used for the rest of the study. To specifically examine motor coordination, the balance beam was used, as it has been used extensively in this and other mouse models of ataxia (Clark *et al.*, 1997; Grusser-Cornehls & Baurle, 2001; Simon *et al.*, 2004; Silva-Fernandes *et al.*, 2010; Teixeira-Castro *et al.*, 2015). At 22 weeks of age, mice were

assessed on the number of foot slips and the latency to cross a wooden beam. On day one of testing, SCA3 water treated mice had more foot slips (wild-type water: 0.2±0.6, SCA3 water: 54.5±24.7, p<0.001) (Figure 4A) and took longer to cross than wild-type water treated mice (wild-type water: 5.2±1.0, SCA3 water: 42.6±22.5, p<0.001) (Figure 4C). Citalopram treatment did not alter wild-type mice performance based on foot slips (wild-type water: 0.2±0.6, wild-type citalopram: 0.4±0.5, p=0.2255) (Figure 4A) or the latency to cross (wild-type water: 5.2±1.0, wild-type citalopram: 5.5±0.9, p=0.2845) (Figure 4C). In contrast, citalopram treated SCA3 mice made fewer foot slips (SCA3 water: 54.5±24.7, SCA3 citalopram: 36.6±19.8, p=0.0404) (Figure 4A) and crossed the beam in less time (SCA3 water: 42.6±22.5, SCA3 citalopram: 24.5±9.1, p=0.0093) (Figure 4C) than SCA3 water treated mice. To validate the improved motor performance in SCA3 mice, SCA3 mice were run three times on test day 2 to obtain an average score, that recapitulated the improved motor coordination in citalopram treated animals with fewer foot slips (SCA3 water: 48.8±18.5, SCA3 citalopram: 25.6±16.1, p=0.0013) (Figure 4B) and a shorter latency to cross (SCA3 water: 34.2±13.3, SCA3 citalopram: 23.1±10.8, p=0.0205) (Figure 4D).

The improved performance could be due to improved motor coordination, or improved strength. To distinguish between these possibilities, we performed two separate assessments of grip strength, the inverted grid and the hanging wire tests. On both assessments, there was no difference between SCA3 water and citalopram treated animals, with wild-type mice performing close to the maximum time allowed for the test of 120s (Inverted grid: SCA3 water: 11.7±8.4, SCA3 citalopram: 14.2±8.1, p=0.3101) (Figure 4E) (Hanging wire: SCA3 water: 26.3±14.5, SCA3 citalopram: 23.7±8.3, p=0.9397) (Figure 4F). Therefore, the improved balance beam performance is likely due to citalopram's actions on motor coordination and not strength.

Cerebellar Purkinje cell firing is partially restored upon citalopram treatment

As SCA3 mice have abnormal Purkinje cell firing, we investigated whether the improved motor coordination detected on the balance beam reflected an improvement in Purkinje cell

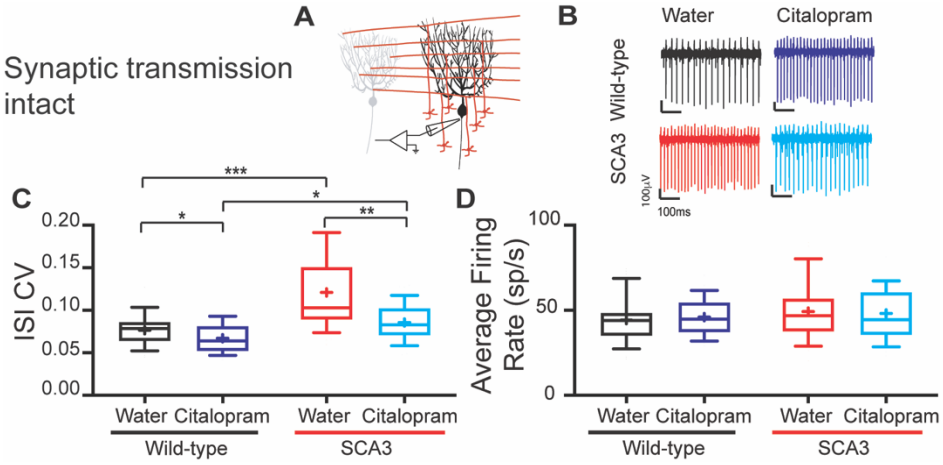

Figure 5: Purkinje cell firing is improved upon citalopram treatment in SCA3. *In Vitro* recordings were performed at 34 weeks of age with synaptic transmission intact (A). Example Purkinje cell intrinsic firing traces from WT (black), SCA3 (red), baseline or citalopram treated (B). Purkinje cells ISI CV (C) is increased in SCA3 in males, as seen in Figure 3, with a decreased ISI CV in SCA3 citalopram mice compared to SCA3 baseline mice. There is no change in firing rate (D-E).
WT N = 3, water n = 32, citalopram n = 29. SCA3 N = 3, water n = 42, citalopram n = 35.

activity. We performed *in vitro* single-unit extracellular recordings as described above from 22-24-week- old SCA3 and wild-type mice, from both the regular drinking water and chronic citalopram administration groups (Figure 5A-B). All experiments were conducted blind to genotype and treatment. When synaptic transmission is intact, similar to what was seen for the female cohort (Figure 3), SCA3 water treated mice had a higher ISI CV compared to wild-type water treated mice (wild-type water 0.0765±0.0183, SCA3 water 0.1210±0.0526, $p<0.001$) (Figure 5C). Interestingly, SCA3 citalopram treated mice had a lower ISI CV compared to SCA3 water treated mice (SCA3 water: 0.1210±0.0526, SCA3 citalopram: 0.0856±0.02121, $p=0.0062$) (Figure 5C).

To determine whether citalopram is alleviating the intrinsic Purkinje cell dysfunction, we repeated the *in vitro* recordings with fast synaptic transmission blocked (Figure 6A-B). While for this cohort the entire dataset only showed a trend to increase the ISI CV when comparing wild-type baseline to SCA3 baseline (wild-type baseline: 0.0522±0.0112, SCA3 baseline: 0.0593±0.0182, $p=0.1453$) (Figure 6C), with our previous data (Figure 3) being based on a large sample size, and with a power analysis confirming we need 110 cells to capture this difference significantly, it is possible that with an increased sample size, this will also reach statistical

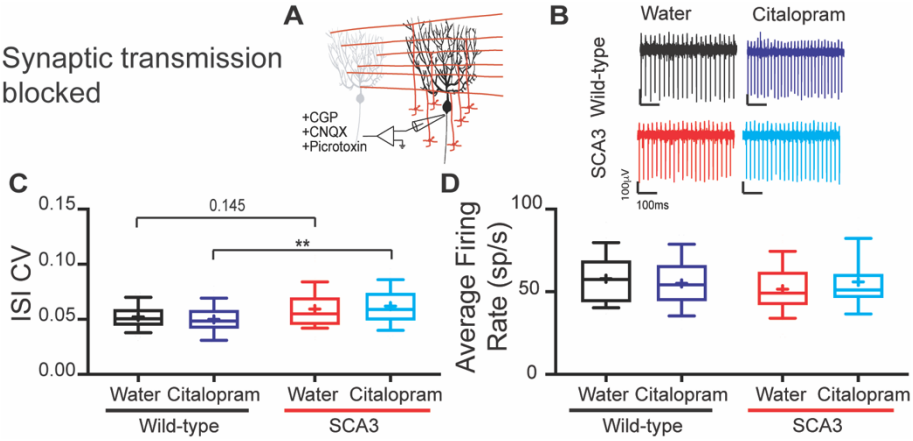

Figure 6: Purkinje cell intrinsic firing is not improved upon citalopram treatment in SCA3. *In Vitro* recordings were performed at 34 weeks of age with fast synaptic transmission blocked (A). Example Purkinje cell intrinsic firing traces from WT (black), SCA3 (red), baseline or citalopram treated (B). Globally, Purkinje cells ISI CV (C) and firing rate (D-E) is not statistically changed.
WT N = 3, water n = 36, citalopram n = 38. SCA3 N = 3, water n = 44, citalopram n = 36

significance (ongoing work). Interestingly, the WT citalopram ISI CV is significantly different from the SCA3 citalopram, and the SCA3 baseline is not significantly different form SCA3 citalopram (wild-type citalopram: 0.0499±0.0131, SCA3 citalopram: 0.0620±0.0167, p=0.0054) (SCA3 baseline: 0.0593±0.0182, SCA3 citalopram: 0.0620±0.0167, p>0.9999) (Figure 6C). Overall, this suggests that the intrinsic irregularity seen in SCA3 is largely not alleviated with chronic citalopram treatment. Instead, citalopram is likely working through the upstream inputs onto Purkinje cells.

DISCUSSION

In this study, we identified DCN and Purkinje cells as novel sites of dysfunction in SCA3 linking altered serotonin signaling to Purkinje cell irregularity in CMVMJD135 SCA3 mice. The Purkinje cell irregularity occurs early on in the disease and is driven by intrinsic and extrinsic factors. Citalopram partially alleviates Purkinje cell dysfunction but does not rescue the intrinsic dysfunction. Hence, we propose that a therapeutic approach that combines citalopram with alleviation of Purkinje cell intrinsic dysfunction will likely further alleviate ataxia in SCA3.

The SCA3 phenotype is a caused by early cerebellar dysfunction and peripheral damage

SCA3 mice have motor incoordination as early as 12 weeks of age, and strength-related behavioral phenotypes previously that are seen as early as 6 weeks. While the behavioral phenotype in SCA3 mice is progressive, the neuronal dysfunction in Purkinje cells and deep cerebellar nuclei appeared to be fairly consistent from 12-60 weeks of age. Based on previous work in our lab, if the cerebellar ataxia worsened, we would expect an increase of irregularity of firing corresponding to symptom severity (Tara *et al.*, 2018). However, unlike pure cerebellar ataxias, in SCA3 the brainstem, spinal cord, muscles, and other brain regions, such as the substantia nigra, are all affected (Woods & Schaumburg, 1972; Rosenberg *et al.*, 1976; Romanul *et al.*, 1977; Stefanescu *et al.*, 2015; Hernandez-Castillo *et al.*, 2018; Koeppen, 2018; Wang *et al.*, 2020). Indeed, in our SCA3 mouse model, it is a combination of these factors that contribute to the presentation of motor symptoms. By 60 weeks of age, mice are unable to properly support their body weight, often pulling their body to move instead of using proper ambulation (Teixeira-Castro *et al.*, 2015) (observational results). This work suggests that early cerebellar dysfunction correlates with ataxia, and alleviating this dysfunction is sufficient to improve motor coordination as assessed by foot slips while crossing the balance beam. Additional studies will be needed to determine if the dysfunctional cerebellum is driving other sites of dysfunction in the central nervous system, or if these other areas undergo independent dysregulation. However, it might also be that the spinal cord/peripheral nervous system related mechanisms of dysfunction arise separately from the cerebellar mechanisms. A combined therapeutic approach will likely be needed to address the many parallel mechanisms driving SCA3 disease.

Neuronal dysfunction as one potential mechanism of SCA3 pathophysiology

There are a few theories underlying SCA3 pathophysiology, ranging from the toxicity of protein aggregates/intranuclear inclusions to extensive cell death. In this SCA3 mouse model, deep cerebellar nuclei present with intranuclear aggregates and degenerate quite late in the disease. At 12 weeks of age, when intranuclear inclusions are not yet visible and there is no cell

death, we observed irregular activity of deep cerebellar nuclei neurons. Furthermore, in SCA3 patients, Purkinje cells show limited degeneration, if at all (Woods & Schaumburg, 1972; Rosenberg *et al.*, 1976; Seidel *et al.*, 2012a; Seidel *et al.*, 2012b). Here, in a model with absence of nuclear inclusions in Purkinje cells, we show that Purkinje cells are dysfunctional since the first stages of disease. In fact, other mouse models of SCA3 have noticed cerebellar neuronal dysfunction, most notably in the YAC mouse model (Cemal *et al.*, 2002; Shakkottai *et al.*, 2011). Together, this strongly suggests that cerebellar Purkinje cell and deep cerebellar nuclei dysfunction is likely a driver of pathophysiology in SCA3 preceding overt degeneration and formation of mutant protein inclusions. This neuronal dysfunction includes a perturbation of intrinsic firing mechanisms, in addition to likely alterations in synaptic transmission.

Citalopram modulates Purkinje cell dysfunction in SCA3

Citalopram, a selective serotonin reuptake inhibitor, improves motor coordination in the SCA3 mouse model (Gunther *et al.*, 2008; Teixeira-Castro *et al.*, 2015). Here we show that citalopram alleviated Purkinje cell dysfunction only when synaptic transmission was intact, but not when fast synaptic transmission was blocked. One potential mechanism of action of this SSRI may be through serotonin's actions on parallel fiber to Purkinje cell synaptic transmission (Lippiello *et al.*, 2016). In addition, as serotonin receptors are expressed throughout the cerebellum, it is also plausible that citalopram acts on cells in the cerebellar circuit upstream of Purkinje cells (Pazos *et al.*, 1985; Pazos & Palacios, 1985; Dieudonne, 2001; Marmolino & Manto, 2010; Oostland & van Hooft, 2013; Oostland *et al.*, 2014). For example, serotonin increases the activity of the inhibitory interneuron Lugaro cells, which then can affect Purkinje cells (Dieudonne, 2001; Dean *et al.*, 2003; Hirono *et al.*, 2012; Fleming & Hull, 2019). Investigating the mechanisms driving cerebellar improvement with citalopram will inform SCA3 pathology and development of targeted therapeutics.

Overall, these results suggest that deep cerebellar nuclei dysfunction, Purkinje cell intrinsic dysfunction and Purkinje cell extrinsic dysfunction are all present in SCA3. By understanding the drivers of cerebellar dysfunction in SCA3, we hope to be able to inform potential mechanisms behind the peripheral and spinal cord dysfunction, in order to develop a multi-faceted approach to treating this complex disease.

METHODS

Animals

Experiments were performed on 12-70 weeks old CMVMJD135 (SCA3) mice bred and genotyped at the Life and Health Science Research Institute, School of Medicine, University of Minho, Braga, Portugal; ICVS/3B's – PT Government Associate Laboratory. Mice were housed at weaning in groups of 5-6 animals in filter-topped polysulfone cages 267 × 207 × 140 mm (370 cm2 floor area) (Tecniplast, Buguggiate, Italy), with corncob bedding (Scobis Due, Mucedola SRL, Settimo Milanese, Italy) in a SPF animal facility. All animals were maintained under standard laboratory conditions: an artificial 12h light/dark cycle (lights on from 8 a.m. to 8 p.m.), with a room temperature of 21±1°C and a relative humidity of 50–60%). Mice were given a standard diet (4RF25 during the gestation and postnatal periods, and 4RF21 after weaning) (Mucedola SRL, Settimo Milanese, Italy) and water ad libitum. Health monitoring was performed according to FELASA guidelines, confirming the Specified Pathogens status of sentinel animals maintained in the same animal room. All procedures were conducted in accordance with European regulations (European Union Directive 86/609/EEC). Animal facilities and the people directly involved in vertebrate animal experiments (S.D.S, A.N.C) as well as coordinating the research (P.M.) were certified by the Portuguese regulatory entity (Direcção Geral de Alimentação e Veterinária). All protocols performed were approved by the Animal Ethics Committee of the Life and Health Sciences Research Institute, University of Minho and by the DGAV (reference 020317).

Mice were shipped to Albert Einstein College of Medicine and allowed at least 2 weeks of recovery

before any experiments were conducted. All experiments were conducted in accordance with the guidelines set by the Institute of Animal Safety and Institute of at Albert Einstein College of Medicine under the senior investigator's (K.K.) Institutional Animal Care and Use Committee approved protocol. Mice were housed on a 12:12 hour reversed light/dark cycle. Mice used in Figures 1-5 had 145±5 CAG repeats, while the citalopram treated animals, Figures 6-8, had 137±5 CAG repeats. Data was analyzed to examine any effect of repeat length on the electrophysiology, with no effect detected. As there has been no reported sex differences in these mice, only female mice were used for Figures 1-5. However, the results were validated in males, as male mice only were used for Figures 6-8.

Behavior

All experiments were performed during the mouse's dark cycle. For all behavior experiments, the experimenter was blinded to the genotype and treatment, where appropriate, of the mice.

Parallel Rod Floor Test: Mice were assessed on the parallel floor rod test for 10-minute sessions, once a day for two days (Kamens *et al.*, 2005; Kamens & Crabbe, 2007). The trials were averaged to obtain total distance traveled and number of foot slips per animal. Ataxia ratio is defined as the number of foot slips (errors) divided by distance traveled (cm).

Disability Score: Mice were assessed using the previously published disability score (Weisz *et al.*, 2005; Tara *et al.*, 2018), as follows: 0 = normal motor behavior; 1 = slightly slowed or abnormal movements; 2 = mild impairments, limited ambulation unless disturbed; 3 = moderate impairment, limited ambulation even when disturbed, frequent abnormal postures; 4 = severe impairment, almost no ambulation, sustained abnormal postures; 5 = prolonged immobility in abnormal postures. To assess the disability score, mice were individually placed in an open field for 30 minutes. The videos were blinded and a 30 second video while the mouse was ambulating was selected and sent to 4 viewers trained on the disability scale and also blind to the conditions of the animal. These 4 scores were averaged to produce a score for each trial. The score for each

mouse was the average of at least 2 trials from separate days.

Balance Beam: Mice were assessed for balance beam performance on a round beam 1m long and scored live. Latency to cross was determined as active crossing time. Foot slips were counted when the hind paws fell ½ way below the side of the beam. 80 slips were considered the maximum number of slips before ending a trial. During treatment, mice were tested on the balance beam using a 1.8cm round 1m beam. At 20-22 weeks, mice were initially tested with one trial on two different beams, 1.8cm and 2.2cm. Based on the tests, a majority of SCA3 mice were unable to perform the 1.8cm beam, and therefore, only data from the 2.2cm beam was used. To validate the single trial results, on day 2, the SCA3 mice were tested three times on the 2.2cm beam, with at least 30 minutes between trials. The three trials were averaged for one score per mouse.

Grip assessment: Grip strength was assessed using the hanging wire test and the inverted grid test. For each test, 120s was the maximum latency to fall. The score for each mouse was reported as the best of 3 trials, separated by at least 5 minutes. The inverted grid test placed a mouse right side up on a metal grid, allowing all 4 limbs to grab the metal grid. The experimenter inverted the grid 180° and measured the latency to fall. The hanging wire test required the mice to grip a rope using only their forepaws to suspend their body. After the experimenter released the mouse, the mouse could use any limb to remain on the rope if able to coordinate to do so. Latency to fall was measured.

Electrophysiology:

***In vivo*:** Mice were implanted with a titanium bracket fixed to the skull with optibond (Kerr Dental) and charisma (Kulzer). A recording chamber was formed on the skull above the cerebellum with dental cement. Craniotomies for recordings were made at the following locations (A/P, M/L): -6.2, ±1.75; and -7, ±0.25. Until time of recording, craniotomies were covered with silicone adhesive (KWIK-SIL, WPI) From awake, head-fixed mice, extracellular single-unit activity was recorded by advancing a tungsten electrode (Thomas Recordings, 2-3 MΩ) until Purkinje cell layers or deep

cerebellar nuclei were detected. Purkinje cells were identified by location, presence of complex spikes, and characteristic firing rate. Deep cerebellar nuclei were identified by location and characteristic firing rate. Signals were filtered (200 Hz-20 kHz) and amplified (2000x) using a custom-built amplifier, and then digitized (20 kHz) using a National Instruments card (PCI-MIO-16-XE) with custom written software in Labview. Waveforms were sorted offline using amplitude, energy, and principal component analysis (Plexon offline sorter).

***In vitro*:** All experiments were conducted blinded to the genotype of the mouse. Mice were anesthetized with isoflurane and rapidly decapitated. The brain was rapidly removed and placed in warm (35±2°C) artificial cerebral spinal fluid (ACSF): (in mM) NaCl 125, KCl 2.5, $NaHCO_3$ 26, NaH_2PO_4 1.25, $MgCl_2$ 1, $CaCl_2$ 2, glucose 11, pH 7.4 when gassed with 5% CO_2:95% O_2. The cerebellum was dissected and 300 µm thick sagittal sections were made using a Campden instruments 7000sz vibratome. Slices were kept in oxygenated ACSF at 35±2°C for 1 hour and then kept at room temperature until use (up to 4 hours). At the time of recording, slices were placed in a recording chamber perfused with warm (35±2°C) ACSF at 1.5 ml/min. Single-unit extracellular recordings were obtained from visually identified Purkinje cells with an upright microscope (Zeiss) using a home-made differential amplifier and glass pipette back-filled with ACSF. Where indicated, to isolate Purkinje cell intrinsic activity, perfusion ACSF contained 10µM Picrotoxin, 1µM CGP55845, and 10µM CNQX to block $GABA_A$, $GABA_B$, and AMPA/Kainate receptors respectively. Signals were digitized (10 kHz) using a National Instruments card (PCI-MIO-16-XE) with custom written software in Labview. Waveforms were sorted offline using amplitude, energy, and principal component analysis (Plexon offline sorter), and output was analyzed using custom written Labview software. For all experiments, each cell was held for a minimum of 5 minutes.

Citalopram treatment

Male and female mice were treated with 8mg/kg citalopram or water starting at 5 weeks of age

for the duration of the study. Citalopram was made fresh on a biweekly. Mice were weighed each week. At 16-19 weeks, mice were shipped to Albert Einstein College of Medicine without citalopram administration for 4-5 days. Immediately upon arrival, mice were continued on the citalopram treatment (8mg/kg in the drinking water) and experiments were conducted after an at least an additional two weeks of reintroduced citalopram treatment.

Statistics

Data is graphed using 10-90 box plots, with the mean indicated by the plus sign. All data was assessed for normalcy, and non-parametric tests were conducted for all datasets that were not normally distributed. T-tests were used for all pair-wise comparisons. Two-way ANOVA as indicated. All data reported in the text as ± standard deviation. * $p<0.05$, ** $p<0.01$, *** $p<0.001$

References

Alvina, K. & Khodakhah, K. (2010a) KCa channels as therapeutic targets in episodic ataxia type-2. *J.Neurosci.*, **30**, 7249-7257.

Alvina, K. & Khodakhah, K. (2010b) The therapeutic mode of action of 4-aminopyridine in cerebellar ataxia. *J.Neurosci.*, **30**, 7258-7268.

Arteaga-Bracho, E.E., Gulinello, M., Winchester, M.L., Pichamoorthy, N., Petronglo, J.R., Zambrano, A.D., Inocencio, J., De Jesus, C.D., Louie, J.O., Gokhan, S., Mehler, M.F. & Molero, A.E. (2016) Postnatal and adult consequences of loss of huntingtin during development: Implications for Huntington's disease. *Neurobiol Dis*, **96**, 144-155.

Ashraf, N.S., Duarte-Silva, S., Shaw, E.D., Maciel, P., Paulson, H.L., Teixeira-Castro, A. & Costa, M.D.C. (2019) Citalopram Reduces Aggregation of ATXN3 in a YAC Transgenic Mouse Model of Machado-Joseph Disease. *Mol Neurobiol*, **56**, 3690-3701.

Barbeau, A., Roy, M., Cunha, L., de Vincente, A.N., Rosenberg, R.N., Nyhan, W.L., MacLeod, P.L., Chazot, G., Langston, L.B. & Dawson, D.M. (1984) The natural history of Machado-Joseph disease. An analysis of 138 personally examined cases. *Can.J.Neurol.Sci.*, **11**, 510-525.

Bishop, G.A. & Ho, R.H. (1985) The distribution and origin of serotonin immunoreactivity in the rat cerebellum. *Brain Res.*, **331**, 195-207.

Cemal, C.K., Carroll, C.J., Lawrence, L., Lowrie, M.B., Ruddle, P., Al-Mahdawi, S., King, R.H., Pook, M.A., Huxley, C. & Chamberlain, S. (2002) YAC transgenic mice carrying pathological alleles of the MJD1 locus exhibit a mild and slowly progressive cerebellar deficit. *Hum Mol Genet*, **11**, 1075-1094.

Clark, H.B., Burright, E.N., Yunis, W.S., Larson, S., Wilcox, C., Hartman, B., Matilla, A., Zoghbi, H.Y. & Orr, H.T. (1997) Purkinje cell expression of a mutant allele of SCA1 in transgenic mice leads to disparate effects on motor behaviors, followed by a progressive cerebellar dysfunction and histological alterations. *The Journal of neuroscience : the official journal of the Society for Neuroscience*, **17**, 7385-7395.

Cook, A.A., Fields, E. & Watt, A.J. (2020) Losing the beat: contribution of Purkinje cell firing dysfunction to disease, and its reversal. *Neuroscience*.

Coutinho, P. & Andrade, C. (1978) Autosomal dominant system degeneration in Portuguese families of the Azores Islands. A new genetic disorder involving cerebellar, pyramidal, extrapyramidal and spinal cord motor functions. *Neurology*, **28**, 703-709.

Darrow, E.J., Strahlendorf, H.K. & Strahlendorf, J.C. (1990) Response of cerebellar Purkinje cells to serotonin and the 5-HT1A agonists 8-OH-DPAT and ipsapirone in vitro. *Eur.J.Pharmacol.*, **175**, 145-153.

Dean, I., Robertson, S.J. & Edwards, F.A. (2003) Serotonin drives a novel GABAergic synaptic current recorded in rat cerebellar purkinje cells: a Lugaro cell to Purkinje cell synapse. *J.Neurosci.*, **23**, 4457-4469.

Dieudonne, S. (2001) Serotonergic neuromodulation in the cerebellar cortex: cellular, synaptic, and molecular basis. *Neuroscientist.*, **7**, 207-219.

Duarte-Silva, S., Neves-Carvalho, A., Soares-Cunha, C., Teixeira-Castro, A., Oliveira, P., Silva-Fernandes, A. & Maciel, P. (2014) Lithium chloride therapy fails to improve motor function in a transgenic mouse model of Machado-Joseph disease. *Cerebellum*, **13**, 713-727.

Esteves, S., Oliveira, S., Duarte-Silva, S., Cunha-Garcia, D., Teixeira-Castro, A. & Maciel, P. (2019) Preclinical Evidence Supporting Early Initiation of Citalopram Treatment in Machado-Joseph Disease. *Mol Neurobiol*, **56**, 3626-3637.

Fleming, E. & Hull, C. (2019) Serotonin regulates dynamics of cerebellar granule cell activity by modulating tonic inhibition. *Journal of neurophysiology*, **121**, 105-114.

Fremont, R., Calderon, D.P., Maleki, S. & Khodakhah, K. (2014) Abnormal high-frequency burst firing of cerebellar neurons in rapid-onset dystonia-parkinsonism. *J. Neurosci.*, **34**, 11723-11732.

Grusser-Cornehls, U. & Baurle, J. (2001) Mutant mice as a model for cerebellar ataxia. *Prog.Neurobiol.*, **63**, 489-540.

Gunther, L., Liebscher, S., Jahkel, M. & Oehler, J. (2008) Effects of chronic citalopram treatment on 5-HT1A and 5-HT2A receptors in group- and isolation-housed mice. *European journal of pharmacology*, **593**, 49-61.

Haines, D.E. & Dietrichs, E. (2012) Chapter 1 - The cerebellum – structure and connections. In Sankara, H.S., Alexandra, D. (eds) *Handbook of Clinical Neurology*. Elsevier, pp. 3-36.

Hansen, S.T., Meera, P., Otis, T.S. & Pulst, S.M. (2013) Changes in Purkinje cell firing and gene expression precede behavioral pathology in a mouse model of SCA2. *Hum Mol Genet*, **22**, 271-283.

Hernandez-Castillo, C.R., King, M., Diedrichsen, J. & Fernandez-Ruiz, J. (2018) Unique degeneration signatures in the cerebellar cortex for spinocerebellar ataxias 2, 3, and 7. *Neuroimage Clin*, **20**, 931-938.

Hirono, M., Saitow, F., Kudo, M., Suzuki, H., Yanagawa, Y., Yamada, M., Nagao, S., Konishi, S. & Obata, K. (2012) Cerebellar globular cells receive monoaminergic excitation and monosynaptic inhibition from Purkinje cells. *Plos One*, **7**, e29663.

Hourez, R., Servais, L., Orduz, D., Gall, D., Millard, I., de Kerchove d'Exaerde, A., Cheron, G., Orr, H.T., Pandolfo, M. & Schiffmann, S.N. (2011) Aminopyridines correct early dysfunction and delay neurodegeneration in a mouse model of spinocerebellar ataxia type 1. *The Journal of neuroscience : the official journal of the Society for Neuroscience*, **31**, 11795-11807.

Hoxha, E., Balbo, I., Miniaci, M.C. & Tempia, F. (2018) Purkinje Cell Signaling Deficits in Animal Models of Ataxia. *Front Synaptic Neurosci*, **10**, 6.

Ito, M. (1984) *The cerebellum and neural control*. Raven Press, New York.

Ito, M., Yoshida, M., Obata, K., Kawai, N. & Udo, M. (1970) Inhibitory control of intracerebellar nuclei by the purkinje cell axons. *Exp.Brain Res.*, **10**, 64-80.

Kamens, H.M. & Crabbe, J.C. (2007) The parallel rod floor test: a measure of ataxia in mice. *Nat Protoc*, **2**, 277-281.

Kamens, H.M., Phillips, T.J., Holstein, S.E. & Crabbe, J.C. (2005) Characterization of the parallel rod floor apparatus to test motor incoordination in mice. *Genes Brain Behav*, **4**, 253-266.

Kawaguchi, Y., Okamoto, T., Taniwaki, M., Aizawa, M., Inoue, M., Katayama, S., Kawakami, H., Nakamura, S., Nishimura, M., Akiguchi, I. & et al. (1994) CAG expansions in a novel gene for Machado-Joseph disease at chromosome 14q32.1. *Nat Genet*, **8**, 221-228.

Kerr, C.W. & Bishop, G.A. (1991) Topographical organization in the origin of serotoninergic projections to different regions of the cat cerebellar cortex. *J.Comp Neurol.*, **304**, 502-515.

Kitzman, P.H. & Bishop, G.A. (1994) The origin of serotoninergic afferents to the cat's cerebellar nuclei. *J.Comp Neurol.*, **340**, 541-550.

Koeppen, A.H. (2018) The Neuropathology of Spinocerebellar Ataxia Type 3/Machado-Joseph Disease. *Adv Exp Med Biol*, **1049**, 233-241.

Lippiello, P., Hoxha, E., Speranza, L., Volpicelli, F., Ferraro, A., Leopoldo, M., Lacivita, E., Perrone-Capano, C., Tempia, F. & Miniaci, M.C. (2016) The 5-HT7 receptor triggers cerebellar long-term synaptic depression via PKC-MAPK. *Neuropharmacology*, **101**, 426-438.

Marmolino, D. & Manto, M. (2010) Past, present and future therapeutics for cerebellar ataxias. *Current neuropharmacology*, **8**, 41-61.

Murano, M., Saitow, F. & Suzuki, H. (2011) Modulatory effects of serotonin on glutamatergic synaptic transmission and long-term depression in the deep cerebellar nuclei. *Neuroscience*, **172**, 118-128.

Oostland, M., Buijink, M.R., Teunisse, G.M., von Oerthel, L., Smidt, M.P. & van Hooft, J.A. (2014) Distinct temporal expression of 5-HT(1A) and 5-HT(2A) receptors on cerebellar granule cells in mice. *Cerebellum*, **13**, 491-500.

Oostland, M. & van Hooft, J.A. (2013) The role of serotonin in cerebellar development. *Neuroscience*, **248**, 201-212.

Palay, S.L. & Chan-Palay, V. (1974) *Cerebellar Cortex: Cytology and Organization*. Springer.

Pazos, A., Cortes, R. & Palacios, J.M. (1985) Quantitative autoradiographic mapping of serotonin receptors in the rat brain. II. Serotonin-2 receptors. *Brain research*, **346**, 231-249.

Pazos, A. & Palacios, J.M. (1985) Quantitative autoradiographic mapping of serotonin receptors in the rat brain. I. Serotonin-1 receptors. *Brain research*, **346**, 205-230.

Person, A.L. & Raman, I.M. (2012) Purkinje neuron synchrony elicits time-locked spiking in the cerebellar nuclei. *Nature*, **481**, 502-505.

Plaitakis, A., Nicklas, W.J. & Berl, S. (1978) Thiamine deficiency: selective impairment of the cerebellar serotonergic system. *Neurology*, **28**, 691-698.

Raman, I.M. & Bean, B.P. (1999) Ionic currents underlying spontaneous action potentials in isolated cerebellar Purkinje neurons. *J.Neurosci.*, **19**, 1663-1674.

Romanul, F.C., Fowler, H.L., Radvany, J., Feldman, R.G. & Feingold, M. (1977) Azorean disease of the nervous system. *N Engl J Med*, **296**, 1505-1508.

Rosenberg, R.N., Nyhan, W.L., Bay, C. & Shore, P. (1976) Autosomal dominant striatonigral degeneration. A clinical, pathologic, and biochemical study of a new genetic disorder. *Neurology*, **26**, 703-714.

Saitow, F., Murano, M. & Suzuki, H. (2009) Modulatory effects of serotonin on GABAergic synaptic transmission and membrane properties in the deep cerebellar nuclei. *Journal of neurophysiology*, **101**, 1361-1374.

Seidel, K., Meister, M., Dugbartey, G.J., Zijlstra, M.P., Vinet, J., Brunt, E.R., van Leeuwen, F.W., Rub, U., Kampinga, H.H. & den Dunnen, W.F. (2012a) Cellular protein quality control and the evolution of aggregates in spinocerebellar ataxia type 3 (SCA3). *Neuropathology and applied neurobiology*, **38**, 548-558.

Seidel, K., Siswanto, S., Brunt, E.R., den Dunnen, W., Korf, H.W. & Rub, U. (2012b) Brain pathology of spinocerebellar ataxias. *Acta Neuropathol*, **124**, 1-21.

Shakkottai, V.G., do Carmo Costa, M., Dell'Orco, J.M., Sankaranarayanan, A., Wulff, H. & Paulson, H.L. (2011) Early changes in cerebellar physiology accompany motor dysfunction in the polyglutamine disease spinocerebellar ataxia type 3. *The Journal of neuroscience : the official journal of the Society for Neuroscience*, **31**, 13002-13014.

Silva-Fernandes, A., Costa Mdo, C., Duarte-Silva, S., Oliveira, P., Botelho, C.M., Martins, L., Mariz, J.A., Ferreira, T., Ribeiro, F., Correia-Neves, M., Costa, C. & Maciel, P. (2010) Motor uncoordination and neuropathology in a transgenic mouse model of Machado-Joseph disease lacking intranuclear inclusions and ataxin-3 cleavage products. *Neurobiol Dis*, **40**, 163-176.

Silva-Fernandes, A., Duarte-Silva, S., Neves-Carvalho, A., Amorim, M., Soares-Cunha, C., Oliveira, P., Thirstrup, K., Teixeira-Castro, A. & Maciel, P. (2014) Chronic treatment with 17-DMAG improves balance and coordination in a new mouse model of Machado-Joseph disease. *Neurotherapeutics*, **11**, 433-449.

Simon, D., Seznec, H., Gansmuller, A., Carelle, N., Weber, P., Metzger, D., Rustin, P., Koenig, M. & Puccio, H. (2004) Friedreich ataxia mouse models with progressive cerebellar and sensory ataxia reveal autophagic neurodegeneration in dorsal root ganglia. *J.Neurosci.*, **24**, 1987-1995.

Stefanescu, M.R., Dohnalek, M., Maderwald, S., Thurling, M., Minnerop, M., Beck, A., Schlamann, M., Diedrichsen, J., Ladd, M.E. & Timmann, D. (2015) Structural and functional MRI abnormalities of cerebellar cortex and nuclei in SCA3, SCA6 and Friedreich's ataxia. *Brain*, **138**, 1182-1197.

Strahlendorf, J.C. & Hubbard, G.D. (1983) Serotonergic interactions with rat cerebellar Purkinje cells. *Brain Res.Bull.*, **11**, 265-269.

Strahlendorf, J.C., Lee, M. & Strahlendorf, H.K. (1984) Effects of serotonin on cerebellar Purkinje cells are dependent on the baseline firing rate. *Exp.Brain Res.*, **56**, 50-58.

Strahlendorf, J.C., Strahlendorf, H.K. & Lee, M. (1986) Enhancement of cerebellar Purkinje cell complex discharge activity by microiontophoretic serotonin. *Exp.Brain Res.*, **61**, 614-624.

Takei, A., Fukazawa, T., Hamada, T., Sohma, H., Yabe, I., Sasaki, H. & Tashiro, K. (2004) Effects of tandospirone on "5-HT1A receptor-associated symptoms" in patients with Machado-Josephe disease: an open-label study. *Clin.Neuropharmacol.*, **27**, 9-13.

Takei, A., Hamada, S., Homma, S., Hamada, K., Tashiro, K. & Hamada, T. (2010) Difference in the effects of tandospirone on ataxia in various types of spinocerebellar degeneration: an open-label study. *Cerebellum*, **9**, 567-570.

Takei, A., Hamada, T., Yabe, I. & Sasaki, H. (2005) Treatment of cerebellar ataxia with 5-HT1A agonist. *Cerebellum.*, **4**, 211-215.

Takei, A., Honma, S., Kawashima, A., Yabe, I., Fukazawa, T., Hamada, K., Hamada, T. & Tashiro, K. (2002) Beneficial effects of tandospirone on ataxia of a patient with Machado-Joseph disease. *Psychiatry Clin.Neurosci.*, **56**, 181-185.

Tara, E., Vitenzon, A., Hess, E. & Khodakhah, K. (2018) Aberrant cerebellar Purkinje cell activity as the cause of motor attacks in a mouse model of episodic ataxia type 2. *Dis Model Mech*, **11**.

Teixeira-Castro, A., Jalles, A., Esteves, S., Kang, S., da Silva Santos, L., Silva-Fernandes, A., Neto, M.F., Brielmann, R.M., Bessa, C., Duarte-Silva, S., Miranda, A., Oliveira, S., Neves-Carvalho, A., Bessa, J., Summavielle, T., Silverman, R.B., Oliveira, P., Morimoto, R.I. & Maciel, P. (2015) Serotonergic signalling suppresses ataxin 3 aggregation and neurotoxicity in animal models of Machado-Joseph disease. *Brain*, **138**, 3221-3237.

Tempia, F., Hoxha, E., Negro, G., Alshammari, M.A., Alshammari, T.K., Panova-Elektronova, N. & Laezza, F. (2015) Parallel fiber to Purkinje cell synaptic impairment in a mouse model of spinocerebellar ataxia type 27. *Front Cell Neurosci*, **9**, 205.

Trouillas, P., Brudon, F. & Adeleine, P. (1988) Improvement of cerebellar ataxia with levorotatory form of 5-hydroxytryptophan. A double-blind study with quantified data processing. *Arch.Neurol.*, **45**, 1217-1222.

Trouillas, P., Xie, J., Adeleine, P., Michel, D., Vighetto, A., Honnorat, J., Dumas, R., Nighoghossian, N. & Laurent, B. (1997) Buspirone, a 5-hydroxytryptamine1A agonist, is

active in cerebellar ataxia. Results of a double-blind drug placebo study in patients with cerebellar cortical atrophy. *Arch.Neurol.*, **54**, 749-752.

Trouillas, P., Xie, J., Getenet, J.C., Adeleine, P., Nighoghossian, N., Honnorat, J., Riche, G. & Derex, L. (1995) [Effect of buspirone, a serotonergic 5-HT-1A agonist in cerebellar ataxia: a pilot study. Preliminary communication]. *Rev.Neurol.(Paris)*, **151**, 708-713.

Walter, J.T., Alvina, K., Womack, M.D., Chevez, C. & Khodakhah, K. (2006) Decreases in the precision of Purkinje cell pacemaking cause cerebellar dysfunction and ataxia. *Nat.Neurosci.*, **9**, 389-397.

Wang, P.S., Wu, Y.T., Wang, T.Y., Wu, H.M., Soong, B.W. & Jao, C.W. (2020) Supratentorial and Infratentorial Lesions in Spinocerebellar Ataxia Type 3. *Front Neurol*, **11**, 124.

Weisz, C.J., Raike, R.S., Soria-Jasso, L.E. & Hess, E.J. (2005) Potassium channel blockers inhibit the triggers of attacks in the calcium channel mouse mutant tottering. *J.Neurosci.*, **25**, 4141-4145.

White, J.J. & Sillitoe, R.V. (2013) Development of the cerebellum: from gene expression patterns to circuit maps. *Wiley Interdiscip Rev Dev Biol*, **2**, 149-164.

Woods, B.T. & Schaumburg, H.H. (1972) Nigro-spino-dentatal degeneration with nuclear ophthalmoplegia. A unique and partially treatable clinico-pathological entity. *J Neurol Sci*, **17**, 149-166.

Zhang, C.Z., Zhuang, Q.X., He, Y.C., Li, G.Y., Zhu, J.N. & Wang, J.J. (2014) 5-HT2A receptor-mediated excitation on cerebellar fastigial nucleus neurons and promotion of motor behaviors in rats. *Pflugers Archiv : European journal of physiology*, **466**, 1259-1271.